

Quantum criticality out of equilibrium in the pseudogap Kondo model

Chung-Hou Chung and Kenneth Yi-Jie Zhang

Electrophysics Department, National Chiao-Tung University, HsinChu, Taiwan, R.O.C.

(Dated: December 6, 2018)

We theoretically investigate the non-equilibrium quantum phase transition in a generic setup: the pseudogap Kondo model where a quantum dot couples to two-left (L) and right (R)-voltage-biased fermionic leads with power-law density of states (DOS) with respect to their Fermi levels $\mu_{L/R}$, $\rho_{c,L(R)}(\omega) \propto |\omega - \mu_{L(R)}|^r$, and $0 < r < 1$. In equilibrium (zero bias voltage) and for $0 < r < 1/2$, with increasing Kondo correlations, in the presence of particle-hole symmetry this model exhibits a quantum phase transition from an unscreened local moment (LM) phase to the Kondo phase. Via a controlled frequency-dependent renormalization group (RG) approach, we compute analytically and numerically the non-equilibrium conductance, conduction electron T-matrix and local spin susceptibility at finite bias voltages near criticality. The current-induced decoherence shows distinct nonequilibrium scaling, leading to new universal non-equilibrium quantum critical behaviors in the above observables. Relevance of our results for the experiments is discussed.

PACS numbers: 72.15.Qm, 7.23.-b, 03.65.Yz

Introduction. Quantum phase transitions (QPTs)[1], the continuous phase transitions occur at zero temperature due to quantum fluctuations, in strongly correlated electron systems have attracted much attention over the last three decades. Near the quantum critical points (QCPs) associated with QPTs, thermodynamic properties exhibit non-Fermi liquid properties and universal scalings. Recently, due to high tunability, nano-devices, such as: quantum dots in the Kondo regime[2, 3], offer a new opportunity to study QPTs. In particular, understanding QPTs in nano-systems under nonequilibrium conditions has become one of the outstanding emergent subjects in condensed matter physics with great fundamental importance[4–6]. In Ref. [5], the authors discovered the distinct non-equilibrium profile in transport near the localized-delocalized QPT of the Kosterlitz-Thouless (KT) type in a generic voltage-biased dissipative resonance-level (quantum dot) from its equilibrium properties at finite temperatures. The current-induced decoherence rate smearing out the transition shows highly non-linear voltage dependence, resulting in these distinct behaviors near QPT.

In this paper, we investigate the non-equilibrium quantum criticality in a different class of generic nano-setup—the pseudogap Kondo (PGK) model[7–11] in a quantum dot[12]. We consider a Kondo quantum dot couples to two-left (L) and right (R)-fermionic leads with a power-law (pseudogap) density-of-states (DOS) which vanishes at the Fermi level $\mu_{L(R)} = \pm V/2$, $\rho_{c,L(R)}(\omega) \propto |\omega - \mu_{L(R)}|^r$ with $0 < r < 1$. Possible realizations of the pseudogap leads include: d -wave superconductors ($r = 1$)[10], graphene[13] ($r = 1$), one-dimensional Luttinger systems ($r > 0$)[8], and quantum dots embedded in a Aharonov-Bohm ring ($r = 2$)[14]. In equilibrium ($V = 0$) and for $0 < r < 1/2$, with decreasing the Kondo couplings the particle-hole (p-h) symmetric PGK model exhibits a “true” QPT (distinct from QPT of the KT type[15]) from the Kondo screened phase to

the unscreened local moment (LM) phase[8, 10]. Near QCP separating these two phases, all observables in equilibrium exhibit universal power-law scalings and have been extensively studied[10, 11]. Nevertheless, there is still lack of understanding regarding their corresponding out-of-equilibrium quantum critical properties. We shall address below this issue with a focus on the universal nonequilibrium scaling behaviors near QCP.

The model and the RG approach. The Hamiltonian of the particle-hole (p-h) symmetric PGK model reads:

$$H = \sum_{k\alpha} (\epsilon_{k\alpha} - \mu_\alpha) c_k^\dagger c_k + \sum_{\alpha, \alpha', k, k', \sigma, \sigma'} J_{\alpha, \alpha'} \mathbf{S}^{dot} \cdot \mathbf{S}_{\alpha' \alpha}^e \quad (1)$$

where $\mathbf{S}^{dot} = f_{\sigma'}^\dagger \tau_{\sigma' \sigma} f_\sigma$, $\mathbf{S}_{\alpha' \alpha}^e = c_{\alpha', k'}^\dagger \tau_{\sigma' \sigma} c_{\alpha, k}$ are the spin-1/2 operators of the electron on the dot and in the leads, respectively, τ are Pauli matrices, and $\alpha, \alpha' = L/R$, $\sigma, \sigma' = \uparrow/\downarrow$ are the lead and spin indices, respectively. $c_{\alpha, k, \sigma}^\dagger$ is the electron creation operator for the lead α with Fermi energies being $\mu_{L/R} = \pm V/2$, and f_σ is the pseudo-fermion operator. The conduction electron leads show power-law (pseudogap) DOS with respect to their Fermi levels $\mu_{L/R}$, $\rho_{c,L(R)}(\omega) \propto |\omega - \mu_{L(R)}|^r$, and $0 < r < 1$. In the Kondo regime, the single-occupancy constraint of the pseudo-fermions is imposed: $\sum_\sigma f_\sigma^\dagger f_\sigma = 1$. Here, the dimensionless inter-lead and intra-lead Kondo couplings are denoted by $g_{LR} = N_0 J_{LR}$, and $g_{LL} = g_{RR} = N_0 J_{LL} = N_0 J_{RR}$, respectively where $N_0 = \frac{1}{2D_0}$ and D_0 is the bandwidth cutoff of the leads. For simplicity, we consider here the symmetrical Kondo couplings: $g_{\alpha\beta} = g$. In equilibrium, the one-loop RG scaling equation for g reads $\frac{\partial g}{\partial \ln D} = rg - 2g^2$ [10]. The critical Kondo coupling $g_c = \frac{r}{2}$ separates the Kondo ($g > g_c$) from the unscreened local moment (LM) phase ($g < g_c$). Much of the equilibrium critical properties can be obtained from the cutoff dependence of the renormalized Kondo coupling: $g^{eq}(D) = \frac{g_c}{1 + (D/T^*)^{-r}}$ with the crossover energy scale being $T^* = D_0 \left(\frac{|g_c - g|}{g_0} \right)^{\frac{1}{r}} \propto |g_c - g|^\nu$ and the cor-

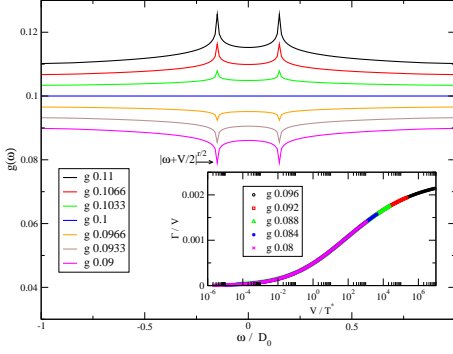


FIG. 1: (Color online) Renormalized Kondo coupling $g(\omega)$ for various bare couplings (in units of D_0) for $r = 0.2$ ($g_c = 0.1$). The bias voltage is $V = 0.3$. Inset: Universal scaling of Γ/V as a function of V/T^* with Γ being the decoherence rate.

relation length exponent being $\nu = 1/r$. At a finite bias voltage, however, the chemical potentials (Fermi levels) of the two leads are shifted by $\pm V/2$. Under various RG approaches, the Kondo interaction vertices in general depend not only on the cutoff scale D , but also on the electron energy (frequency)[16, 18]. We employ here a weak coupling 1-loop frequency-dependent RG approach of Ref. [5, 16] which keeps track of energy of the incoming electrons. For $r = 0$ our results agree excellently with those via a more sophisticated functional RG approach in Ref.[19]. Note that our weak coupling theory for the p-h symmetric model Eq. 1 works well only for $r \rightarrow 0$. The QCP between LM and Kondo phases disappears for $r \geq 1/2$, and our theory breaks down for r near 1[10]. Note also that the above p-h symmetric QCP is stable against p-h asymmetry for $0 < r < r^* = 0.375$ [10]. We therefore restrict ourselves to the p-h symmetric model for simplicity. The scaling equation for the Kondo couplings of our model under this approach reads[16, 19]:

$$\frac{\partial g(\omega)}{\partial \ln D} = \sum_{\beta=-1,1} \tanh\left(\frac{D}{2T}\right) \left[\frac{r}{2} g(\omega) - g^2(\omega) \right] \Theta\left(D - \left| \omega + \frac{\beta V}{2} + i\Gamma \right| \right) \quad (2)$$

$$\Gamma = \pi \sum_{\alpha\alpha'} \int d\omega f_{\omega}^{\alpha} (1 - f_{\omega}^{\alpha'}) g^2(\omega), \quad (3)$$

where Γ is the current-induced decoherence rate obtained from the imaginary part of the pseudofermion self-energy[16], $f_{\omega}^{\alpha} = \frac{1}{e^{\frac{\omega - \mu_{\alpha}}{T}} + 1}$ is the Fermi function of the α lead and $k_B = \hbar = e = 1$. Note that in equilibrium at a finite temperature T the RG flows of the Kondo couplings are cut off by T ; while as within the nonequilibrium RG approach they are cutoff by $\Gamma \ll V$, a much lower energy scale than V [16]. Distinct critical behaviors are therefore expected[5]. We shall focus below on what these distinct nonequilibrium quantum critical behaviors are.

We first solve Eq. 2 and Eq. 3 for $g(\omega)$ self-consistently at

$T = 0$. As shown in Fig. 1, for $g > (<)g_c$, the renormalized Kondo couplings exhibit peaks (dips) at $\omega = \pm V/2$, indicating Kondo (local moment) phase; while $g(\omega)$ is completely flat at criticality $g = g_c$. The qualitative nature of these peaks (dips) in $g(\omega)$ agree well with Ref. [5, 6] as signatures of conducting (insulating) behavior. The height (depth) of the peaks (dips) get shorter (shallower) as one reaches to QCP from the Kondo (LM) phase. We restrict ourselves to the LM phase ($g \leq g_c$) where the perturbative RG approach is controlled. The full analytical solution for $g(\omega)$ in the LM phase in the limit of $D \rightarrow 0$ is found to be:

$$\begin{aligned} g(\omega) &= g + g_1(\omega) + g_2(\omega), \\ g_1(\omega) &= \frac{g_0(1 + \tilde{V}^r)(|\tilde{\omega} - \frac{\tilde{V}}{2}|^r - 1)}{2(1 + \tilde{V}^r)(1 + |\tilde{\omega} - \frac{\tilde{V}}{2}|^r)} \Theta(\tilde{D}_0 - |\tilde{\omega} - \frac{\tilde{V}}{2}|) \\ &\quad + \frac{g_c(\tilde{V}^r - |\tilde{\omega} - \frac{\tilde{V}}{2}|^r)}{2(1 + \tilde{V}^r)(1 + |\tilde{\omega} - \frac{\tilde{V}}{2}|^r)} \Theta(\tilde{V} - |\tilde{\omega} - \frac{\tilde{V}}{2}|) \\ &\quad + (\omega \rightarrow -\omega), \\ g_2(\omega) &= \left(\frac{g_c \tilde{V}^{\frac{r}{2}}}{1 + \tilde{V}^r} \right) \left\{ \frac{\tilde{V}^{\frac{r}{2}} - |\tilde{\omega} - \frac{\tilde{V}}{2}|^{\frac{r}{2}}}{1 + \tilde{V}^{\frac{r}{2}} |\tilde{\omega} - \frac{\tilde{V}}{2}|^{\frac{r}{2}}} \right. \\ &\quad \times [\Theta(\tilde{\Gamma} - |\tilde{\omega} - \frac{\tilde{V}}{2}|) - \Theta(\tilde{D}_0 - |\tilde{\omega} - \frac{\tilde{V}}{2}|)] \\ &\quad \left. + \frac{\tilde{\Gamma}^{\frac{r}{2}} - \tilde{V}^{\frac{r}{2}}}{1 + (\tilde{V}\tilde{\Gamma})^{\frac{r}{2}}} \Theta(\tilde{\Gamma} - |\tilde{\omega} - \frac{\tilde{V}}{2}|) \right\} \\ &\quad + (\omega \rightarrow -\omega) \end{aligned} \quad (4)$$

with $\tilde{V} = \frac{V}{T^*}$, $\tilde{\omega} = \frac{\omega}{T^*}$, $\tilde{D}_0 = \frac{D_0}{T^*}$, $\tilde{\Gamma} = \frac{\Gamma}{T^*}$, and g_0 being the bare Kondo coupling. The peaks (dips) of $g(\omega)$ near $\omega = \pm V/2$ shows a power-law behavior: $|g(\omega) - g(\omega = \pm V/2)| \propto |\omega \mp \frac{V}{2}|^{\frac{r}{2}}$ with a width of Γ . We furthermore find analytically via Eq. 4 the universal scaling forms for $g(\omega = 0, V)$, and $g(\omega = \pm V/2, V)$. These properties will be used in the following analysis to determine various novel nonequilibrium scaling behaviors in the LM phase:

$$g(\omega = 0) = \frac{g_c}{1 + (\frac{V}{2T^*})^{-r}}, g(\omega = \frac{V}{2}) = \frac{g_c}{1 + (\frac{V}{T^*})^{-\frac{r}{2}}}. \quad (5)$$

Nonequilibrium decoherence. The current-induced decoherence Γ which cuts off the RG flow is the key to understand nonequilibrium quantum criticality of the model as all nonequilibrium observables depend crucially on the scaling behavior of Γ . As shown in Fig.1 (Inset), Γ/V in the LM phase exhibits perfect universal V/T^* scaling over a wide range $10^{-6} < V/T^* < 10^6$. We believe this slow crossover which extends over many decades is likely related to the large correlation length exponent $\nu = 1/r$ of the model. To gain more insight, we obtain analytical approximated form: $\Gamma/\pi \approx (1 - \frac{\pi}{4})Vg^2(\omega = \frac{V}{2}) + \frac{\pi}{4}Vg^2(\omega = 0)$ where $g(\omega)$ is well approximated by a semi-ellipse for $-V/2 < \omega < V/2$ (see excellent agreement in Fig. 2 (c) between dotted and dashed lines)[5].

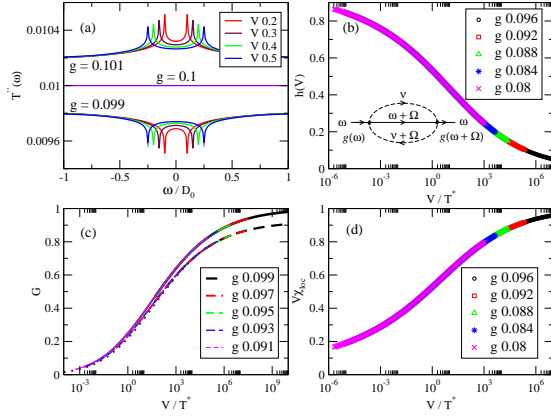


FIG. 2: (Color online) (a). The imaginary part of the T-matrix $T''(\omega)$ (in unit of $\frac{3\pi}{8N(0)}$) versus V/T^* at $T = 0$. (b). $h(V)$ defined in Eq. 9 versus V/T^* . Inset: the diagram for the T-matrix. (c). The $T = 0$ nonequilibrium conductance $G(V)$ (solid lines) normalized to $\frac{3\pi g_c^2}{4}$ in the LM phase versus V/T^* shows distinct scaling from the equilibrium counterpart, $G^{eq}(T \rightarrow V)$ (dashed lines). The dotted line is the analytical form via Eq. 11. (d). The scaling of $V\chi_{loc}$ versus V/T^* with χ_{loc} being the local impurity susceptibility. The bare Kondo couplings in (a), (b), (c), and (d) are in unit of D_0 , and $r = 0.2$.

Via Eq. 5 the decoherence Γ at $T = 0$ is approximated as:

$$\frac{\Gamma}{\pi V} \approx (1 - \frac{\pi}{4}) \frac{g_c^2}{[1 + (\frac{V^2}{T^{*2}} \frac{\Gamma}{V})^{-\frac{r}{2}}]^2} + \frac{\pi}{4} \frac{g_c^2}{[1 + (\frac{V}{2T^*})^{-r}]^2} \quad (6)$$

It is clear from Eq. 6 that Γ/V is an universal scaling function of V/T^* . This well explains the scaling behavior obtained numerically (see Fig. 1 Inset). We extract further the asymptotic power-law behaviors of Γ/V as a function of V/T^* . For $\Gamma \ll V \ll T^*$, we have $\frac{\Gamma}{\pi V} \approx \frac{\pi g_c^2}{4} (\frac{V}{2T^*})^{2r}$. For $V \gg \Gamma \gg T^*$, however, we find $\frac{\Gamma}{\pi V} \approx \frac{\pi g_c^2}{4} [1 - 2(\frac{V}{2T^*})^{-r}]$. At criticality, $\Gamma = \pi g_c^2 V$. The scaling behavior of the decoherence Γ (Fig. 2 and Eq. 6), leading to distinct nonequilibrium scaling behaviors of all the observables discussed below, is our central result.

The conduction electron T-matrix. First, we analyze nonequilibrium critical properties from the conduction electron T-matrix, defined by $G_{\alpha,\alpha',\sigma}^{R(0)} = G_{\alpha,\sigma}^{R(0)} \delta_{\alpha,\alpha'} + G_{\alpha,\sigma}^{R(0)} T_{\alpha,\alpha',\sigma}(\omega) G_{\alpha',\sigma}^{R(0)}(\omega)$ [10, 11] with $G_{\alpha,\alpha',\sigma}^{R(0)}$, $G_{\alpha,\sigma}^{R(0)}$ being the full and bare conduction electron Green's function, respectively. The imaginary part of T-matrix $Im[T(\omega)] \equiv T''(\omega)$ is directly proportional to the experimentally measurable tunneling density of states (TDOS) of our setup. Via renormalized perturbation theory up to second order (see Fig. 2 (b) Inset), we have

$$T_{\alpha\alpha'}^<(\omega) = \sum_{\beta=L,R} \int d\Omega g(\omega) g(\omega+\Omega) [\chi^R(\Omega) \tilde{G}_{\beta}^< + \chi^<(\Omega) \tilde{G}_{\beta}^A] \quad (7)$$

where $\chi(\Omega) = \int_{-\infty}^{\infty} dt e^{i\Omega t} \chi(t)$ with $\chi(t) \equiv -\langle T_c \{ \mathbf{S}^{dot}(t) \cdot \mathbf{S}^{dot}(0) \} \rangle$ are impurity susceptibilities, $\tilde{G}_{\beta}^{<(A)}$ corresponds to the lesser (advanced) component of the conduction electron Green's functions with constant (DOS) (the effect of the pseudogap leads has been taken into account by the renormalized coupling $g(\omega)$), and $T_{\alpha\alpha'}^>(\omega) = T_{\alpha\alpha'}^<(-\omega)$. The imaginary part of the T-matrix at $T = 0$ is hence given by:

$$-\pi T_{\alpha\alpha'}''(\omega) = \frac{3\pi^2}{8N(0)} g^2(\omega), \quad (8)$$

in agreement with the result in Ref. [20] via a different perturbative RG approach to the multi-channel Kondo model out of equilibrium. For $V = T = 0$, $T''(\omega)_{\alpha\alpha'}$ in the LM phase exhibits a power-law dip at $\omega = 0$, $T''(\omega) \propto |\omega|^{\frac{r}{2}}$. For $V > 0$, this dip is splitted into two at $\omega = \pm \frac{V}{2}$ with the same power-law: $T''(\omega) - T''(\omega = V/2) \propto |\omega - \frac{V}{2}|^{\frac{r}{2}}$. At the dips of $T''(\omega = \pm V/2)$, we find $T''(\omega = V/2) \propto g^2(\omega = V/2)$ shows a distinct nonequilibrium scaling behavior as a function of V/T^* compared to that in equilibrium form $T''(\omega = 0) \propto g^2(\omega = 0)$. To extract this different scaling behavior more clearly, we define the effective depth of the dips for $T''(\omega = \pm V/2)$, estimated as:

$$h(V) \equiv \left| \frac{T''(\omega = V/2) - T''(\omega = 0)}{T''(\omega = 0)} \right| = \left| 1 - \frac{g^2(\omega = V/2)}{g^2(\omega = 0)} \right| \quad (9)$$

It is clear from Eq. 9 that in the LM phase $h(V)$ follows an universal scaling function of V/T^* (see Fig. 2 (b)), and has the following asymptotic behaviors: $h(V) \approx 1 - (\frac{4\Gamma}{V})^r$ for $\Gamma \ll V \ll T^*$; while for $T^* \ll \Gamma \ll V$, $h(V) \approx 2[(\frac{V\Gamma}{T^{*2}})^{-\frac{r}{2}} - (\frac{V}{2T^*})^{-r}]$. The new nonequilibrium scaling function $h(V)$ is detectable via STM measurement.

The nonequilibrium conductance. Next, we turn our attention to the transport. The nonequilibrium current I via the Fermi-Gordon rule reads[5, 16]:

$$I = \frac{3\pi}{4} \int d\omega \left[\sum_{\sigma} g_{LR}(\omega)^2 f_{\omega}^L (1 - f_{\omega}^R) \right] - (L \leftrightarrow R). \quad (10)$$

The current I is computed numerically by Eq. 10, and is approximated as[5]: $I \approx \frac{3\pi}{4} [(1 - \frac{\pi}{4}) V g^2(\omega = \frac{V}{2}) + \frac{\pi}{4} V g^2(\omega = 0)]$. The differential conductance is readily obtained numerically via $G = \frac{\partial I}{\partial V}$. In the LM phase, it has the analytical approximated form:

$$G(V) \approx \frac{3\pi g_c^2}{4} (1 - \frac{\pi}{4}) \frac{[1 + (1+r) (\frac{V\Gamma}{T^{*2}})^{-\frac{r}{2}}]}{[1 + (\frac{V\Gamma}{T^{*2}})^{-\frac{r}{2}}]^3} + \frac{3\pi^2 g_c^2}{16} \frac{[1 + (1+2r) (\frac{V}{2T^*})^{-r}]}{[1 + (\frac{V}{2T^*})^{-r}]^3} \quad (11)$$

As shown in Fig. 2 (c), for $T^* \ll V \ll D_0$, $G(V)$ ap-

proaches the equilibrium scaling form

$$G^{eq}(V \rightarrow T) \approx \frac{3\pi}{4} g^{eq}(T)^2 = \frac{\frac{3\pi}{4} g_c^2}{[1 + (T/T^*)^{-r}]^2} \quad (12)$$

; while as for $V/T^* \gg 1$ it exhibits a distinct universal scaling behavior of V/T^* . The perfect scaling behavior of $G(V/T^*)$ is a direct consequence of the V/T^* scaling in Γ/V . By contrast, the universal V/T^* scaling is absent in Ref.[5] as Γ/V is not a universal function of V/T^* there. For $\Gamma \ll V \ll T^*$, the conductance behaves as: $G(V) \approx [a(\frac{V}{2T^*})^{2r} + b(\frac{V}{T^*})^{2r+2r^2}]$ with $a = \frac{3\pi^2 r^2}{64}$, $b = \frac{3\pi r^2}{16}(1 - \frac{\pi}{4})(\frac{r^2}{8})^r$, which shows a prefactor reduction in the first term $\propto V^{2r}$ with respect to its equilibrium form $G^{eq}(V \rightarrow T \ll T^*) \approx \frac{3\pi r^2}{16}(\frac{T}{T^*})^{2r}$ and a sub-leading correction with an anomalous power-law behavior $\propto V^{2r+2r^2}$. For $V \gg \Gamma \gg T^*$, however, we find $G(V) \approx \frac{3\pi^2 r^2}{64}[1 - p(\frac{V}{2T^*})^{-r} - q(\frac{V}{T^*})^{-2r}]$ with $p = 1 - r$ and $q = \frac{\pi}{8}(1 - \frac{\pi}{4})(1 - r)(\frac{r^2}{8})^{-\frac{r}{2}}$, which deviates significantly from its equilibrium form $G^{eq}(V \rightarrow T \gg T^*) \approx \frac{3\pi r^2}{16}[1 - 2(\frac{T}{T^*})^{-r}]$. It is worthwhile emphasizing that due to the very different role played by the bias V and temperature T , $G(V)$ follows a completely different scaling function from its equilibrium form $G^{eq}(V \rightarrow T)$ over the full range of V/T^* (see Eq. 11 and Eq. 12) though it tends to converge with its equilibrium form for $V \ll T^*$.

Local spin susceptibility. We furthermore analyze the scaling behaviors of the local spin susceptibility $\chi_{loc}(V) \equiv \frac{\partial M}{\partial h}|_{h \rightarrow 0}$ in the LM phase with h being a small magnetic field, M being the magnetization $M = \frac{n_{\uparrow} - n_{\downarrow}}{n_{\uparrow} + n_{\downarrow}}$. Following Ref. [5, 6, 16], for $V \gg h \rightarrow 0$, we find $M \approx \frac{\int_{-\frac{V}{2}}^{\frac{-V+h}{2}} d\omega g^2(\omega)}{\int_{-\frac{V}{2}}^{\frac{V}{2}} d\omega g^2(\omega)}$. The approximated form for $V\chi_{loc}$ reads

(see Fig. 2 (d))[17]: $V\chi_{loc} \approx \frac{g(\omega=V/2)^2}{\frac{\pi}{4}g(\omega=0)^2 + (1-\frac{\pi}{4})g(\omega=V/2)^2}$. For $\Gamma \ll V \ll T^*$, χ_{loc} exhibits an anomalous power-law behavior: $\chi_{loc} \propto \frac{1}{V^{1-\eta_{\chi}}}$ with $\eta_{\chi} = 2r^2$, distinct from its equilibrium constant behavior: $T\chi_{loc}(T \ll T^*) \propto (g_c - g)^r$ [11]. For $V \gg \Gamma \gg T^*$, however, we find the local susceptibility acquires a power-law correction to the Curie behavior: $V\chi_{loc} \approx 1 - V\Delta\chi_{loc}$ and $\Delta\chi_{loc} \propto \frac{1}{V^{1-\Delta\eta_{\chi}}}$ with an anomalous exponent $\Delta\eta_{\chi} = -r$; while as its corresponding equilibrium form shows a different anomalous power-law behavior: $\chi_{loc}(T \gg T^*) \propto \frac{1}{T^{1-\eta_{\chi}}}$ with $\eta_{\chi} = r^2$ [10, 11]. At criticality ($g = g_c$), χ_{loc} shows perfect Curie law behavior: $\chi_{loc} \propto 1/V$. These distinct nonequilibrium signatures near QCP are detectable in local susceptibility measurement.

Conclusions. In summary, via a controlled frequency-dependent renormalization group approach we have investigated the quantum phase transition out of equilibrium in the pseudogap Kondo quantum dot. At zero temperature and finite bias voltage, we discovered in the local moment phase the new quantum critical behaviors in the T-matrix, conductance, and local spin suscepti-

bility that are distinct from those in equilibrium and at finite temperatures. The key to explain these differences lies in the fact that the current-induced decoherence at a finite bias voltage (out of equilibrium) acts quite differently from that at a finite temperature but zero bias (in equilibrium), resulting in distinct nonequilibrium behavior near the quantum phase transition. Our predictions open up a new perspective both theoretically and experimentally in the study of the Kondo dot coupled to exotic leads with pseudogap density of states.

We thank M. Vojta for many helpful discussions. This work is supported by the NSC grant No.98-2112-M-009-010-MY3, the MOE-ATU program, the NCTS of Taiwan, R.O.C. .

-
- [1] S. Sachdev, *Quantum Phase Transitions*, Cambridge University Press (2000); S. L. Sondhi, S. M. Girvin, J. P. Carini, and D. Shahar, Rev. Mod. Phys. **69**, 315 (1987).
 - [2] R. M. Potok, I. G. Rau, H. Shtrikman, Y. Oreg and D. Goldhaber-Gordon, Nature **447** 167-171 (2007).
 - [3] A.C. Hewson, *The Kondo Problem to Heavy Fermions*, Cambridge University Press, Cambridge (1997).
 - [4] D. E. Feldman, Phys. Rev. Lett., **95**, 177201 (2005); A. Mitra, S. Takei, Y.B. Kim, and A. J. Millis, Phys. Rev. Lett., **97**, 236808 (2006); S. Takei, Y.B. Kim, Phys. Rev. B **76** 115304 (2007); S. Kirchner, Q.M. Si, Phys. Rev. Lett. **103**, 206401 (2009).
 - [5] C.-H. Chung, K. Le Hur, M. Vojta and P. Wölfle, Phys. Rev. Lett. **102**, 2106803 (2009).
 - [6] C.H. Chung, K.V.P. Latha, K. Le Hur, M. Vojta and P. Wölfle, Phys. Rev. B, **82**, 115325 (2010).
 - [7] D. Withoff, E. Fradkin, Phys. Rev. Lett. **64**, 1835 (1990).
 - [8] C. Gonzalez-Buxton and K. Ingersent, Phys. Rev. B **57**, 14254 (1998).
 - [9] K. Ingersent and Q. Si, Phys. Rev. Lett. **89**, 076403 (2002).
 - [10] M. Vojta and L. Fritz, Phys. Rev. B **70**, 094502 (2004); L. Fritz and M. Vojta, Phys. Rev. B **70**, 214427 (2004).
 - [11] Lars Fritz, Serge Florens, Matthias Vojta, Phys. Rev. B **74**, 144410 (2006).
 - [12] John Hopkinson, Karyn Le Hur, Emilie Dupont, Physica B, **359-361** 1454 (2005).
 - [13] Matthias Vojta, Lars Fritz, Ralf Bulla, Eur. Phys. Lett. **90**, 27006 (2010).
 - [14] Luis G. G. V. Dias da Silva, Nancy Sandler, Pascal Simon, Kevin Ingersent, Sergio E. Ulloa, Phys. Rev. Lett. **102** 166806 (2009).
 - [15] The crossover scale T^* associated with the “true” QPT is a power-law function of the distance $t = |g - g_c|$ to QCP; while as it depends exponentially on t for QPT of the KT type.
 - [16] A. Rosch, J. Paaske, J. Kroha, P. Wölfle, Phys. Rev. Lett. **90**, 076804 (2003); J. Phys. Soc. Jpn. **74**, 118 (2005).
 - [17] J. Paaske, A. Rosch, Phys. Rev. B **69** 155330 (2004); Chung-Hou Chung, K.V.P. Latha, Phys. Rev. B **82**, 085120 (2010).
 - [18] S. Kehrein, Phys. Rev. Lett. **95**, 056602 (2005); H. Schoeller, F. Reininghaus, Phys. Rev. B **80**, 045117 (2009); S.G. Jakobs, V. Meden and H. Schoeller, Phys. Rev. Lett. **99**, 150603 (2007).

- [19] H. Schmidt and P. Wöelfle, Ann. Phys. (Berlin) **19**, No. 1-2, 60-74 (2010). [20] A. Mitra, A. Rosch, Phys. Rev. Lett. **106** 106402, (2011).